Biochimica et Biophysica Acta 1807 (2011) 251–261

Contents lists available at ScienceDirect

Biochimica et Biophysica Acta

journal homepage: www.elsevier.com/locate/bbabio

A novel subfamily of mitochondrial dicarboxylate carriers from *Drosophila melanogaster*: Biochemical and computational studies

Domenico Iacopetta [a,1], Marianna Madeo [a,1], Gianluca Tasco [b], Chiara Carrisi [c], Rosita Curcio [a], Emanuela Martello [a], Rita Casadio [b,*], Loredana Capobianco [c,*], Vincenza Dolce [a,*]

[a] Department of Pharmaco-Biology, University of Calabria, Arcavacata di Rende, 87036 Cosenza, Italy
[b] Biocomputing Group, Department of Biology, University of Bologna, Italy
[c] Department of Biological and Environmental Sciences and Technologies, University of Salento, 73100 Lecce, Italy

ARTICLE INFO

Article history:
Received 16 June 2010
Received in revised form 13 November 2010
Accepted 21 November 2010
Available online 3 December 2010

Keywords:
Mitochondria
Proteomics
Drosophila melanogaster
Dicarboxylate carrier
CG8790
CG4323
CG11196
CG18363

ABSTRACT

The dicarboxylate carrier is an important member of the mitochondrial carrier family, which catalyzes an electroneutral exchange across the inner mitochondrial membrane of dicarboxylates for inorganic phosphate and certain sulfur-containing compounds. Screening of the *Drosophila melanogaster* genome revealed the presence of a mitochondrial carrier subfamily constituted by four potential homologs of mammalian and yeast mitochondrial dicarboxylate carriers designated as *Dm*Dic1p, *Dm*Dic2p, *Dm*Dic3p, and *Dm*Dic4p. In this paper, we report that *Dm*DIC1 is broadly expressed at comparable levels in all development stages investigated whereas *Dm*DIC3 and *Dm*DIC4 are expressed only in the pupal stage, no transcripts are detectable for *Dm*DIC2. All expressed proteins are localized in mitochondria. The transport activity of *Dm*Dic1-3-4 proteins has been investigated by reconstitution of recombinant purified protein into liposomes. *Dm*Dic1p is a typical dicarboxylate carrier showing similar substrate specificity and inhibitor sensitivity as mammalian and yeast mitochondrial dicarboxylate carriers. *Dm*Dic3p seems to be an atypical dicarboxylate carrier being able to transport only inorganic phosphate and certain sulfur-containing compounds. No transport activity was observed for *Dm*Dic4p. The biochemical results have been supported at molecular level by computing the protein structures and by structural alignments. All together these results indicate that *D. melanogaster* dicarboxylate carriers form a protein subfamily but the modifications in the amino acids sequences are indicative of specialized functions.

1. Introduction

The selective transport of specific essential metabolites across the mitochondrial membrane is mediated by nuclear encoded carriers, which form the mitochondrial carrier family (MCF). All carriers share some common properties, including a tripartite structure made up of a 3 tandemly repeated sequence of about 100 amino acids in length, the presence of six hydrophobic domains that span the mitochondrial membrane as α-helices, and the presence of a conserved sequence motif [1]. An analysis of the *Drosophila melanogaster* genome revealed the presence of 46 mitochondrial carriers [2]. So far, several *D. melanogaster* mitochondrial carriers have been identified by their high similarity with orthologs in other organisms. They have been characterized as the two isoforms of the ADP/ATP translocase [3,4], the brain uncoupling protein [5], the carnitine/acylcarnitine [6], the citrate [2], the mitoferrin [7], and the thiamine pyrophosphate [8] carriers. However, the transport functions of most members of this family are still unknown. For example, the dicarboxylate carrier (Dic) is an important member of MCF, which catalyzes an electroneutral exchange across the inner mitochondrial membrane of dicarboxylates (e.g., malonate, malate, succinate) for inorganic phosphate and certain sulfur-containing compounds (e.g., sulfite, sulfate, thiosulfate) [9–13]. The Dic has been broadly investigated. It has been purified from both rat [14,15] and yeast [16] mitochondria and kinetically characterized in isolated mitochondria [9–13], as well as following functional reconstitution of the mitochondrial purified protein [17,18] and of the recombinant proteins overexpressed in *Escherichia coli* [19–21]. In mammals, this carrier plays an important role in gluconeogenesis, urea synthesis, and sulphur metabolism [22], whereas in yeast, it is believed to have an anaplerotic function [23]. Despite the

Abbreviations: HEPES, (4-(2-hydroxyethyl)-1-piperazineethanesulfonic acid); RT-PCR, reverse transcription polymerase chain reaction; SDS-PAGE, polyacrylamide gel electrophoresis in the presence of sodium dodecyl sulfate

* Corresponding authors. V. Dolce is to be contacted at Department of Pharmaco-Biology, University of Calabria, Rende 87036 (CS), Italy. Tel.: +39 0 984493177; fax: +39 0 984493270. L. Capobianco, Department of Biological and Environmental Sciences and Technologies, University of Salento, 73100 Lecce, Italy. Tel.: +39 0 832298864; fax: +39 0 832298626. R. Casadio, Department of Biology, University of Bologna, Italy. Tel.: +39 0 512094005; fax: +39 0 51242576.
E-mail addresses: casadio@biocomp.unibo.it (R. Casadio), loredana.capobianco@unile.it (L. Capobianco), vdolce@unical.it (V. Dolce).
[1] These authors contributed equally to this work.

0005-2728/$ – see front matter © 2010 Elsevier B.V. All rights reserved.
doi:10.1016/j.bbabio.2010.11.013

numerous and important functions in higher eukaryotes and yeast, only one protein isoform has been found.

A phylogenetic analysis of the *D. melanogaster* mitochondrial carriers with the known carriers in mammals and yeast showed the presence of numerous subfamilies in the *D. melanogaster* genome, one of these included four proteins related to dicarboxylate carrier. In this paper, the four gene products of CG8790, CG4323, CG11196, and CG18363 *D. melanogaster* genes, henceforth called *Dm*Dic1p, *Dm*Dic2p, *Dm*Dic3p, and *Dm*Dic4p, respectively, have been identified. These proteins are respectively 280, 304, 287, 302 amino acids long and possess the characteristics of the MCF [1]. The *Dm*Dic1p and *Dm*Dic3p were overexpressed in *E. coli*, purified, reconstituted into phospholipidic vesicles, and identified by their transport and kinetic properties. Furthermore, the different functional behavior was further detailed at a molecular level by computing the protein structures and by structural alignments. Results highlight relevant structural and compositional features responsible of the different transport selectivity. This is the first time that a dicarboxylate carrier subfamily has been identified at the molecular level.

2. Materials and methods

2.1. Sequence search and analysis

The Flybase database (www.fruitfly.org) was screened with the sequence of human DIC [24] using blastp. The amino acid sequences were aligned with ClustalW (www.ebi.ac.uk/Tools/clustalw2/index.html).

2.2. Bacterial expression and purification of DmDic proteins

Total RNA was extracted from Oregon R adult flies and pupal using RNeasy Mini Kit (Qiagen, Milan, Italy) and reverse transcribed as described in Ref. [25]. The coding sequences of *Dm*DIC1, *Dm*DIC3, and *Dm*DIC4 were amplified from the respective transcripts (CG8790-RA, CG11196-RA, and CG18363-RA) by PCR. Forward and reverse primers corresponding to the DIC coding sequences were synthesized with additional *Nde*I and *Hin*dIII sites, respectively (*Dm*DIC1 forward 5′-TAGCATATGCCCCACCAAGAGAGAAAATC-3′, and reverse 5′-CTAAAGCTTATTCAAGGTGCCAAACTTGAGACG-3′; *Dm*DIC3 forward 5′-TAGCATATGGGAGAAGACAGTTCGAGGC-3′, and reverse 5′-CTAAAGCTTCTTGTCAGGTGGCAGATATCCAA-3′; and *Dm*DIC4 forward 5′- TAGCATATGCCGGTTTTTGATGACCACTT-3′, reverse 5′-CTAAAGCTTATTGTACTTCTCCCCTCCCAGGG-3′). The product was cloned into the *Nde*I–*Hin*dIII sites of the modified expression vector pET-21b/V5-His [2]. Transformants of *E. coli* TG1 cells were selected and screened. The absence of the stop codon in the reverse primer sequence led to the expression of *Dm*Dic proteins with a carboxy-terminal V5- and His6-epitope tags. *Dm*Dic proteins were overexpressed in *E. coli* in BL21 (DE3). Inclusion bodies were isolated and purified by centrifugation and Ni^{+}-NTA-agarose affinity chromatography as described [26].

2.3. Reconstitution into liposomes and transport assays

The recombinant proteins in sarkosyl were reconstituted into liposomes in the presence or absence of substrates, as described before [27]. External substrate was removed from proteoliposomes through Sephadex G-75 columns, pre-equilibrated with 50 mM NaCl and 10 mM HEPES at pH 7.0 (buffer A). Transport at 25 °C was started by adding L-[1,4(2,3)-^{14}C]malate (Amersham, Milan, Italy) or [^{33}P] phosphate (BCS BIOTECH, Cagliari, Italy) to substrate-loaded proteoliposomes (exchange) or to empty proteoliposomes (uniport). In both cases, transport was terminated by the addition of 50 mM pyridoxal 5′-phosphate and 30 mM bathophenanthroline [27]. In controls, the inhibitors were added at the beginning together with the radioactive substrate. All transport measurements were performed at the same internal and external pH values (10 mM HEPES, pH 7.0). Finally, the external substrate was removed and the radioactivity in the liposomes was measured [27]. The experimental values were corrected by subtracting control values. The initial transport rate was calculated from the radioactivity of proteoliposomes after 20 s (in the initial linear range of substrate uptake). The reconstituted proteins were also assayed for other transport activities.

2.4. Expression analysis by RT-PCR

Total RNA isolated from wild-type Oregon R embryos, larvae, pupae, and adult flies was reverse transcribed with the Gene Amp RNA PCR Core kit (PerkinElmer Life Sciences, Monza, Italy) using random hexamers as primers (final volume, 40 μl). The fragments corresponding to the isoforms of *Dm*DIC were amplified by 30 cycles of PCR in a final volume of 50 μl containing 200 nM of both forward and reverse primers. As a control, a 368-bp ribosomal protein 49 (RP49) fragment was amplified with the same conditions described above. The specific primers for each amplified fragment were CG8790-RA sense CACCGGCATGACATAACACAGCC and antisense GCTTGAATCCCTCCTGGCGGTAG; CG8790-RB sense CACCCGGAAAACCAGAGGCAG and antisense GCTTGAATCCCTCCTGGCGGTAG; CG4323 sense CGAATCGATCAGCTTAGTTGAGACAGGTA and antisense GCGTGCTTATAGTTGCGCCTCTTC; CG11196 sense CCAAGAAATTAAGTTCGGTCTATGGGAGA and antisense CTTTGTAGATGCGGAAAAGGCCG; CG18363 sense ATGCCGGTTTTTGATGACCACTTC and antisense CATCCGCACGTTAATCAGATCCG. The PCR amplified products were analyzed as previously reported [8].

2.5. Computational methods

The location of repeats of ketoacids and phosphate carriers sequences were retrieved from UniProtKB (http://www.uniprot.org), while repeats of *Dm*Dics were computed with PFAM (http://pfam.sanger.ac.uk/) based on a HMM model of the mitochondrial transporters as derived from the ADP/ATP carrier. Repeat multiple alignments were generated with ClustalW (http://www.ebi.ac.uk/Tools/clustalw2/), and the outputs were colored according the zappo color scheme of the Jailview tool (http://www.jalview.org/). Profile–profile alignments were computed with the corresponding option of ClustalW.

Difference in steric hindrances was calculated considering side chain volume values as reported (http://www.imb-jena.de/IMAGE_AA.html). Position of transmembrane helices of *Dm*Dics along the protein sequence was predicted with the program ENSEMBLE (www.biocomp.unibo.it, [28]). The program is based on Neural Networks and Hidden Markov models and scores with a per-protein accuracy of 90% and 71% for topography and topology prediction, respectively [28]. Three-dimensional (3D) models of *Dm*Dic proteins were computed with the program Modeller version 9.7 [29] after structural alignment of the transmembrane regions of target with those of the template sequence. The template is the bovine ADP/ATP carrier (ADT1_BOVIN, pdb code 1OKC, Resolution 2.20 Å) [30] whose sequence shares less than 20% of identical residues with all the *Dm*Dic targets. The structural alignment was manually constrained considering secondary structure and known conserved motifs. For a given alignment, 15 model structures were built and evaluated with the programs Procheck [31] and Prosa [32] for stereochemically and energetic validation, respectively. Only the best evaluated model was retained after the procedure for *Dm*Dic1p, *Dm*Dic3p, and *Dm*Dic4p.

Overlapping of the OGC and *Dm*Dics was realized by Multiprot3D (http://bioinfo3d.cs.tau.ac.il/MultiProt/) and visualized by chimera (http://www.cgl.ucsf.edu/chimera/). Residues involved in matrix and cytoplasmic network were extracted from structural multiple alignments.

2.6. Other methods

Proteins were analysed by SDS/PAGE and stained with Coomassie Blue dye. The amount of recombinant pure *Dm*Dic proteins was estimated by laser densitometry of stained samples, using carbonic anhydrase as protein standard [26]. The amount of proteins incorporated into liposomes were measured as described in Ref. [26] and varied between 25 and 30% of the protein added to the reconstitution mixture.

3. Results

3.1. Identification of DmDIC cDNAs

The protein sequence of the human DIC (hDIC), encoded by the SLC25A10 gene [24], was used to query Flybase database for homologous *D. melanogaster* sequences. Six full-length clones encoding for a DIC-related sequences were found. The clones NM_142022 and NM_169510 are two 5′-UTR splice variants of the CG8790 gene and encode for an identical polypeptide of 280 amino acids long (named *Dm*Dic1p) with a calculated molecular mass of 30.7 kDa. The clones NM_169896 and NM_169897 are two 5′-UTR splice variants of CG4323 gene and encode for the same polypeptide of 304 amino acids long (named *Dm*Dic2p) with a calculated molecular mass of 33.5 kDa. The clone NM_136500, the transcript of the gene CG11196, encodes for a polypeptide of 287 amino acids long (named *Dm*Dic3p) with a calculated molecular mass of 31.2 kDa. The clone NM_140797, the transcript of gene CG18363, encodes for a polypeptide of 302 amino acids long (named *Dm*Dic4p) with a calculated molecular mass of 33.9 kDa. The pairwise alignment of these polypeptides reveals 57% identity and 71% similarity with hDIC for *Dm*Dic1p, 46% identity and 64% similarity for *Dm*Dic2p, 45% identity and 65% similarity for *Dm*Dic3p, and 35% identity and 57% similarity for *Dm*Dic4p (data not shown). All four *Dm*Dic proteins belong to the MCF due to their tripartite structure, the presence of two hydrophobic regions in each repeat and the threefold repetition of the signature motif. A phylogenetic analysis (data not shown) carried out using the *Dm*Dic1-4p and the di- and tricarboxylates mitochondrial carriers sequences from man and yeast as well as those of the uncoupling proteins revealed that *Dm*Dic1-4p are monophyletic and form a group with all Dic proteins.

3.2. Expression analysis of DmDICs in different developmental stages

To determine the expression levels of transcripts corresponding to CG8790, CG4323, CG1196, and CG18363 genes, we performed a semi-quantitative RT-PCR analysis on total RNAs from wild-type embryos, larvae, pupae, and adults, using primers based on the sequence retrieved from Flybase database. A PCR product of the predicted size was detected at high levels in all developmental stages analyzed (Fig. 1) for transcripts CG8790-RA and CG8790-RB. No visible band of expression was found for the CG4323-RA and CG4323-RB transcripts; moreover, any attempt to amplify the coding sequence corresponding to the CG4323 transcripts failed (data not shown). A PCR product of the predicted size was detected at high levels only in the pupal stage for transcripts CG1196-RA and CG18363-RA (Fig. 1). A control RT-PCR was carried out using specific primers for RP49 (Fig. 1).

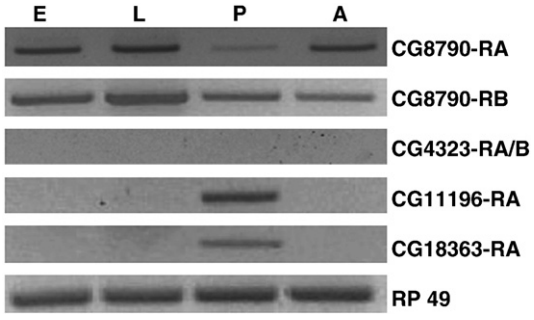

Fig. 1. Expression of the *Dm*DIC transcripts during development. Ethidium bromide staining of the RT-PCR products obtained using specific primers for *D. melanogaster* DICs transcripts and cDNA from Oregon R embryos (E), larvae (L), pupae (P), and adults (A). RP49 was amplified as a control for RNA integrity.

3.3. Bacterial expression of the DmDic proteins

The *Dm*Dic1p, *Dm*Dic3p, and *Dm*Dic4p were overexpressed at high levels in *E. coli* BL-21 (DE3) as inclusion bodies and were purified by Ni^{+}-NTA-agarose affinity chromatography (Fig. 2 lanes 3, 5, and 7, panel A). The identity of the purified proteins was confirmed by Western blot analysis (Fig. 2 lanes 3, 5, and 7, panel B). Approximately 100–150 mg of each purified protein per liter of culture was obtained. No protein overexpression was detected in bacteria carrying the vector lacking of the *Dm*DICs coding sequence harvested before (data not shown) and after (Fig. 2, lane 1) induction of expression.

3.4. DmDic1p is a typical dicarboxylate carrier

Proteoliposomes reconstituted with recombinant *Dm*Dic1p catalyzed an exchange of external [^{14}C]malate for internal phosphate, which was inhibited completely by a mixture of pyridoxal 5′-phosphate and bathophenanthroline. They did not catalyze homoexchanges for pyruvate, carnitine, glutamine, and ornithine (internal concentration 20 mM; external concentration 1 mM). Furthermore, no [^{14}C]malate/phosphate exchange activity was detected if *Dm*Dic1p was boiled before incorporation into liposomes nor by the reconstitution of sarkosyl-solubilized material from bacterial cells either lacking the expression vector for *Dm*Dic1p or in cells harvested immediately before induction of expression.

The substrate specificity of *Dm*Dic1p was investigated in greater detail by measuring the uptake of [^{14}C]malate and of [^{33}P]phosphate into proteoliposomes that had been preloaded with a variety of substrates (Table 1). In the absence of internal substrate, the uptake of labeled malate or phosphate was not observed. The highest activities of [^{14}C]malate and [^{33}P]phosphate uptake into proteoliposomes were detected with internal malate, phosphate, malonate, and maleate. Succinate, sulfate, and thiosulfate were exchanged to a low extent for external

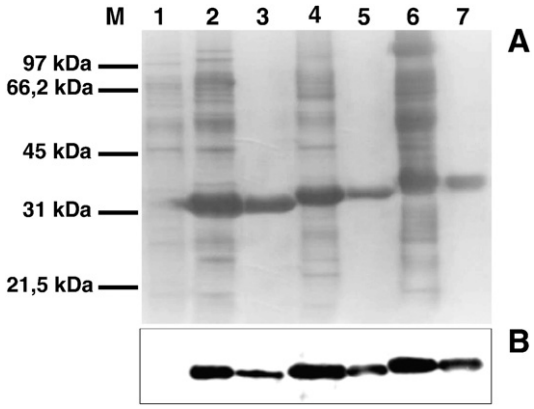

Fig. 2. Purification of the recombinant *Dm*Dic proteins by $Ni2^{+}$-NTA-agarose affinity chromatography. Proteins were separated by 12.5% SDS-PAGE and stained with Coomassie Blue dye (A) or transferred to nitrocellulose and immunodecorated with mouse anti-V5 monoclonal antibody (B). Lanes M, markers (Phosphorylase b, Serum albumin, Ovalbumin, Carbonic anhydrase, Trypsin inhibitor); *E. coli* BL21(DE3) containing the expression vector without the DICs coding sequence (panels A and B lane 1); *E. coli* BL21(DE3) containing the expression vector with the DIC1-3-4 coding sequences, respectively (panels A and B lanes 2, 4, and 6); purified *Dm*Dic1-3-4p from bacteria shown in lanes 2, 4, and 6, respectively (panels A and B lanes 3, 5, and 7). Samples were taken 3 h after induction. The same number of bacteria was analyzed in each sample.

Table 1
Substrate specificity of the recombinant *Dm*Dic1p in reconstituted liposomes. Proteoliposomes reconstituted with the *Dm*Dic1p were preloaded internally with various substrates (concentration 20 mM). Transport was started by the external addition of 1 mM [^{14}C]malate or 2 mM ^{33}P. Transport was measured over 60 s. The activity of the malate/malate exchange was 33.4 μmol/min × mg protein. The activity of the phosphate/phosphate exchange was 30.47 μmol/min × mg protein. Similar results were obtained in five different experiments.

Internal substrate (20 mM)	[^{14}C] Malate % activity	^{33}Pi % activity
None (Cl^-)	0.5 ± 0.03	0.7 ± 0.04
L-malate	100 ± 9.78	105 ± 9.89
Phosphate	65 ± 5.98	100 ± 8.80
Malonate	86 ± 7.50	103 ± 9.40
Maleate	58 ± 4.50	72 ± 6.50
Succinate	33 ± 2.65	77 ± 6.58
Sulfate	30 ± 2.54	80 ± 7.40
Thiosulfate	38 ± 2.20	63 ± 4.90
Oxalacetate	27 ± 1.95	32 ± 2.80
2-Oxoglutarate	3 ± 0.15	1.1 ± 0.03
Aspartate	2.3 ± 0.08	0.2 ± 0.01
Citrate	2 ± 0.12	1.8 ± 0.08
Fumarate	1.4 ± 0.07	1.4 ± 0.05
Phenylsuccinate	0.7 ± 0.01	1 ± 0.01
Glutathione (reduced)	0.2 ± 0.01	0.4 ± 0.02
Glutathione (oxidized)	0.2 ± 0.02	0.7 ± 0.03

malate and to high extent for external phosphate. To a somewhat lower extent oxalacetate was exchanged for both external substrates. Virtually no exchange was observed with internal 2-oxoglutarate, aspartate, citrate, fumarate, phenylsuccinate, reduced glutathione, and oxidized glutathione. Similar to the biochemically characterized Dic proteins from various organisms [19–21], the proteoliposomes reconstituted with the *D. melanogaster* recombinant *Dm*Dic1p import external malate and phosphate only in exchange for certain dicarboxylates, inorganic sulfur-containing anions, and phosphate.

The effects of inhibitors on the [^{14}C]malate/phosphate exchange reaction catalyzed by the reconstituted *Dm*Dic1p were also examined. The exchange reaction was inhibited by the substrate analogues 10 mM butylmalonate (91%), 10 mM benzylmalonate (95%), 10 mM phenylsuccinate (54%), as well as by the inhibitors 10 mM bathophenanthroline (97%) and 10 mM pyridoxal 5′-phosphate (98%). Butylmalonate was a more effective inhibitor of the [^{14}C]malate/phosphate exchange as for the rat Dic protein in mitochondria [12]. Inhibitors of other characterized mitochondrial carriers, such as 0.1 mM carboxyatractyloside (15%) and 10 mM 1,2,3-benzenetricarboxylate (2%), had no effect on the activity of the *D. melanogaster* reconstituted protein. The sulphydryl reagents were not tested since cysteine residues are not present in the primary structure. The transport characteristics of the *Dm*Dic1p and the effects of inhibitors on transport parallel those determined previously for the dicarboxylate carrier in mitochondria [9,11,12,18] and are identical after Dic protein purification from mitocondria and reconstitution into liposomes [15,17] as well as with the reconstituted recombinant Dic protein [19–21]. The kinetic constants of the recombinant purified *Dm*Dic1p were determined by measuring the initial transport rate at various external, [^{14}C]malate or [^{33}P]phosphate concentrations in the presence of a constant saturating internal concentration of the same substrate (homo-exchange). The half-saturation constant (*Km*) for phosphate is about three times higher than for malate; in liposomes reconstituted with the *D. melanogaster* protein, the mean values from six experiments are 0.81 ± 0.1 mM and 2.35 ± 0.3 mM for malate and phosphate, respectively. Thus, *Dm*Dic1p is also similar to the rat recombinant Dic (*Km* values for malate and phosphate are 0.78 mM and 1.77 mM, respectively) [19], whereas the *Km* values of the recombinant yeast Dic for malate and phosphate are 0.59 mM and 1.65 mM, respectively [20]. In six experiments, the *Dm*Dic1p V_{max} value, corrected for small differences in efficiency of reconstitution, is 64 ± 2.5 μmol/min × mg protein. This value is virtually the same for both the malate/malate and phosphate/phosphate exchanges and is independent of the type of substrate, as previously observed [9,18–20]. Furthermore, the V_{max} value of the recombinant *D. melanogaster* protein is higher than those determined previously for the purified rat liver and recombinant yeast Dic [18,20]. This difference may arise because the efficiency of reconstitution was not quantified in the earlier studies.

3.5. DmDic3p is an atypical dicarboxylate carrier

*Dm*Dic3p was reconstituted into liposomes, and its transport activity was tested in homo-exchange experiments. Using external and internal substrate concentrations of 1 and 20 mM, respectively, the reconstituted protein catalyzed an active [^{33}P]phosphate/phosphate exchange, but surprisingly not a homo-exchange for malate.

The substrate specificity of *Dm*Dic3p was investigated in greater detail by measuring the uptake of [^{33}P]phosphate into proteoliposomes preloaded with a variety of substrates (Table 2). In the absence of internal substrate, the uptake of labeled phosphate was not observed. The highest activities of [^{33}P]phosphate uptake into proteoliposomes were detected with internal phosphate, sulfate, and thiosulfate. Virtually no exchange was observed with the other internal substrates tested (Table 2). In contrast to the *Dm*Dic1p and to the other biochemically characterized Dic proteins [19–21], the proteoliposomes reconstituted with the *Dm*Dic3p import external phosphate only in exchange for inorganic sulfur-containing anions and phosphate.

The effects of inhibitors on the [^{14}C]malate/phosphate exchange reaction catalyzed by the reconstituted *Dm*Dic3p were also examined. The exchange reaction was inhibited by 10 mM bathophenanthroline (87%) and 10 mM pyridoxal 5′-phosphate (91%) and by the sulphydryl reagents 0.1 mM mersalyl (95%) and 0.1 mM *N*-ethylmaleimmide (53%). Inhibitors of other characterized mitochondrial carriers, such as 0.1 mM carboxyatractyloside (7%) and 10 mM 1,2,3-benzenetricarboxylate (5%), had no effect on the activity of the *D. melanogaster* reconstituted protein. The transport characteristics of the *Dm*Dic3p and the effects of inhibitors on transport are very different from those determined for *Dm*Dic1p (see above) and those determined previously for the dicarboxylate carriers [9,11,12,15,17–21].

The kinetic constants of the recombinant purified *Dm*Dic3p were determined by measuring the initial transport rate at different external [^{33}P]phosphate concentrations in the presence of a constant saturating internal concentration of the same substrate (homo-exchange). The half-saturation constant (*Km*) for phosphate is 3.2 ± 0.2 mM. In six

Table 2
Substrate specificity of the recombinant *Dm*Dic3p in reconstituted liposomes. Proteoliposomes reconstituted with the *Dm*Dic3p were preloaded internally with various substrates (concentration 20 mM). Transport was started by the external addition of 2 mM ^{33}P. Transport was measured over 60 s. The activity of the phosphate/phosphate exchange was 95.2 μmol/min × mg protein. Similar results were obtained in five different experiments.

Internal substrate (20 mM)	^{33}Pi % activity
None (Cl^-)	0.5 ± 0.03
Phosphate	100 ± 7.00
Sulfate	145 ± 11.2
Thiosulfate	69 ± 5.03
L-malate	6 ± 0.23
Malonate	5 ± 0.20
Succinate	15 ± 0.90
Phenylsuccinate	13 ± 0.95
2-Oxoglutarate	0.6 ± 0.03
Fumarate	0.4 ± 0.01
Maleate	4 ± 0.36
Aspartate	7 ± 0.57
Oxalacetate	8 ± 0.47
Citrate	2.4 ± 0.18
Glutathione (reduced)	0.3 ± 0.02
Glutathione (oxidized)	0.8 ± 0.05

experiments, the V_{max} value, corrected for small differences in efficiency of reconstitution, is 253 ± 3.5 μmol/min × mg protein.

3.6. DmDic4p does not exhibit carrier activity

*Dm*Dic4p was reconstituted into liposomes, and its transport activity was tested in homo-exchange experiments. In our conditions using external and internal substrate concentrations of 1 and 20 mM, respectively, the reconstituted protein did not catalyze an active exchange for [^{14}C]malate/malate or [^{33}P]phosphate/phosphate. Furthermore, no uptake of sulfate, succinate, 2-oxoglutarate, pyruvate, citrate, ADP, ATP, alanine, glycine, valine, methionine, aspartate, glutamate, or glutamine was observed, nor an uptake of any of these compounds into proteoliposomes containing internal malate or phosphate and vice versa (data not shown).

3.7. Structural analysis of the different DmDic proteins

The *Dm*Dic set of sequences at hand was analyzed in relation to structural conservation with mitochondrial carriers. As suggested by Robinson et al. [33], a source of information is the conservation of symmetry-related triplets in the three typical repeats that characterise each sequence within the superfamily. Here we focus on the extent of conservation of structural important regions in the *Dm*Dic set of sequences in relation to the correspondent regions in the ATP/ADP carrier. Specifically we would like to classify our sequences whose functional role is described above within the functional transporter families.

In Fig. 3A, the three repeats typical of the mitochondrial carriers evaluated in the *Dm*Dics with the PFAM HHM model are aligned towards the same regions in all the ketoacid transporters, including the bovin OGC (M2OM_BOVIN). In Fig. 3B, the same is done considering the aligned repeats of some typical and well-described mitochondrial phosphate carriers including one from *D. melanogaster*, Q9XZE4_DROME (MPCP_DROME). In the figures, the symmetry-related triplets of each sequence can be read vertically. According to the legend of Fig. 3A, the color code highlights relevant physico-chemical characteristics of the lateral side chain, and helps in grasping major conserved properties among orthologue sequences. Also, given the multiple alignment with the bovin ADP/ATP carrier of known structure a topological location of the different residues is possible. The fundamental assumption here is therefore that all the mitochondrial carriers of eukaryotes are folding with the same fold. This has been discussed at length, and the results of several mutagenesis experiments combined with functional and structural analysis seem to confirm the assumption [34–36].

Profile–profile alignments of our *Dm*Dic set with the ketoacid carriers (including OGC) and with the phosphate carriers score 434 and 271, respectively. This finding ensures that the set of *Dm*Dics under study can be better classified within the ketoacid than within the phosphate transporters that include, for the sake of comparison, also Q9XZE4_DROME from the same organisms.

In *Dm*Dics, a more detailed analysis in terms of functional relevant residues can be done by comparing with functionally characterized bovine mitochondrial oxoglutarate carrier (OGC), whose functional relevant residues have been determined after point mutations. The comparison among structural/functional characteristics of OGC and the ADP/ATP carrier has been detailed elsewhere [34,35]. Here we will focus on the comparison among what is known for OGC and its projection on the *Dm*Dic models in order to highlight specific regions of interest at the molecular level in the *Dm*Dic carriers (*Dm*Dic1p vs. OGC = 36.5%, *Dm*Dic3p vs. OGC = 30.6%, *Dm*Dic4p vs. OGC = 27.4%). All the models, including that of OGC, have been computed adopting as a template the only mitochondrial carrier known so far with atomic resolution [30] (Fig. 4A and B).

Most of the functional important residues in OGC have been determined by cysteine replacement and subsequent modification by sulphydryl reagents on the initial rate of uptake of 2-oxoglutarate. After multiple sequence/structural alignment of the ADP/ATP carrier, OGC and the three *Dm*Dic proteins under investigation we can conclude (Figs. 3A, 4A and B): (i) all the primary sequences (including that of the template) are made up of three tandemly repeated homologous domains comprising of about 100 residues; (ii) the characteristic conserved sequence motif (P-X[DE]-X-X-[RK]) is present at the C terminus of Helix 1 (H1) and Helix 5 (H5), and only partially conserved in Helix 3 (H3) of OGC and this is also common to the three *Dm*Dic proteins under investigation (Fig. 3A); (iii) all the *Dm*Dic sequences are modelled on the ADP/ATP carrier satisfying all the protein structural constraints that allow a model to be included among those of a real fold (the resulting structure is a six alpha-helical bundle with a 3-fold pseudo-symmetry, as shown in Fig. 4A); (iv) the models are overlapping with few differences in some of the exposed loops in the matrix and cytoplasmic regions (Fig. 4B). Similarly to OGC, all the *Dm*Dic sequences in the matrix network are stabilized by two salt bridges. One hydrogen bond is present in *Dm*Dics; however, it is not detected in OGC. In the cytoplasmic network, three salt bridges can stabilize the structure, whereas in OGC, one salt bridge and two hydrogen bonds are present. The apparent rigidity is conserved in all the three *Dm*Dics, suggesting a possible strict exchange mechanism [33]; (v) by direct comparison, the same substrate binding site can be deduced (Figs. 3A and 4A). This is based also on previous observations highlighting a common substrate binding site for the different 2-oxoglutarate and malate substrates. The result was derived by considering residues conservation and chemical constraints; the binding site occurs in the water filled cavity of the carrier (Fig. 3A, columns highlighted in grey) and substrate specificity can be due to the different side chains around the three specific highly conserved contact points (contact residues); (vi) for all the carriers, the proline of the signature motif kinks the transmembrane helices by bringing their terminal ends together at the base of the carrier cavity allowing overall conformational changes during substrate exchange.

In the light of all the above observations supported by results shown in Figs. 3A and 4A and B, we can now describe the common major similarities/differences for the *Dm*Dic1-3-4p under investigation. This allows a correlation of the residues conservation/substitution with the functional results described above and obtained after reconstitution of the expressed proteins in liposomes. Contact points relevant to substrate binding are highlighted in red in Fig. 4A. Their labelling as contact points 1, 2, and 3 is taken from a previous study trying to identify essential residues involved in binding of the different substrates in the water exposed binding pocket of the different mitochondrial carriers [35,37]. In Fig. 3A, all the contact points are highlighted with white fields. In Table 3, the more important residues in OGC and their position relative to the corresponding ones in the *Dm*Dic1-3-4p chains are listed along with the details of their experimental annotations.

Contact point 1 (CP1) in alpha Helix 2 (H2) of OGC includes residues from R90 to R98, with a tyrosine (Y) in position 94. The key residues of the motif (R, Y, and R) are conserved in *Dm*Dic1p and *Dm*Dic3p, the typical and atypical dicarboxylate carriers, respectively (see also Fig. 3A for comparison with hortologues). In *Dm*Dic4p, OGC Y94 is replaced by S (S86) and OGC R98 by H (H90), suggesting that the loss of conserved residues in these positions is relevant to the lack of activity of this carrier (Fig. 3A). As to contact point 2 (CP2) in alpha Helix 4 (H4), R190 of OGC is similarly conserved in the typical and atypical *Dm*Dic proteins with the exception of *Dm*Dic4p (K179). This corroborates the view that R in this position is crucial in modulating activity also in the *Dm*Dic protein subfamily. Interestingly the flanking OGC A191 is conserved in *Dm*Dic3p (A169) and not in *Dm*Dic1p (G165). Contact point 3 (CP3) in alpha Helix6 (H6) is conserved in all sequences (R288 in OGC, R257, R261, and R272 in DmDic1-3-4p, respectively).

Some interesting considerations are at hand considering that *Dm*Dic3p as compared to *Dm*Dic1p is an atypical carrier, since as

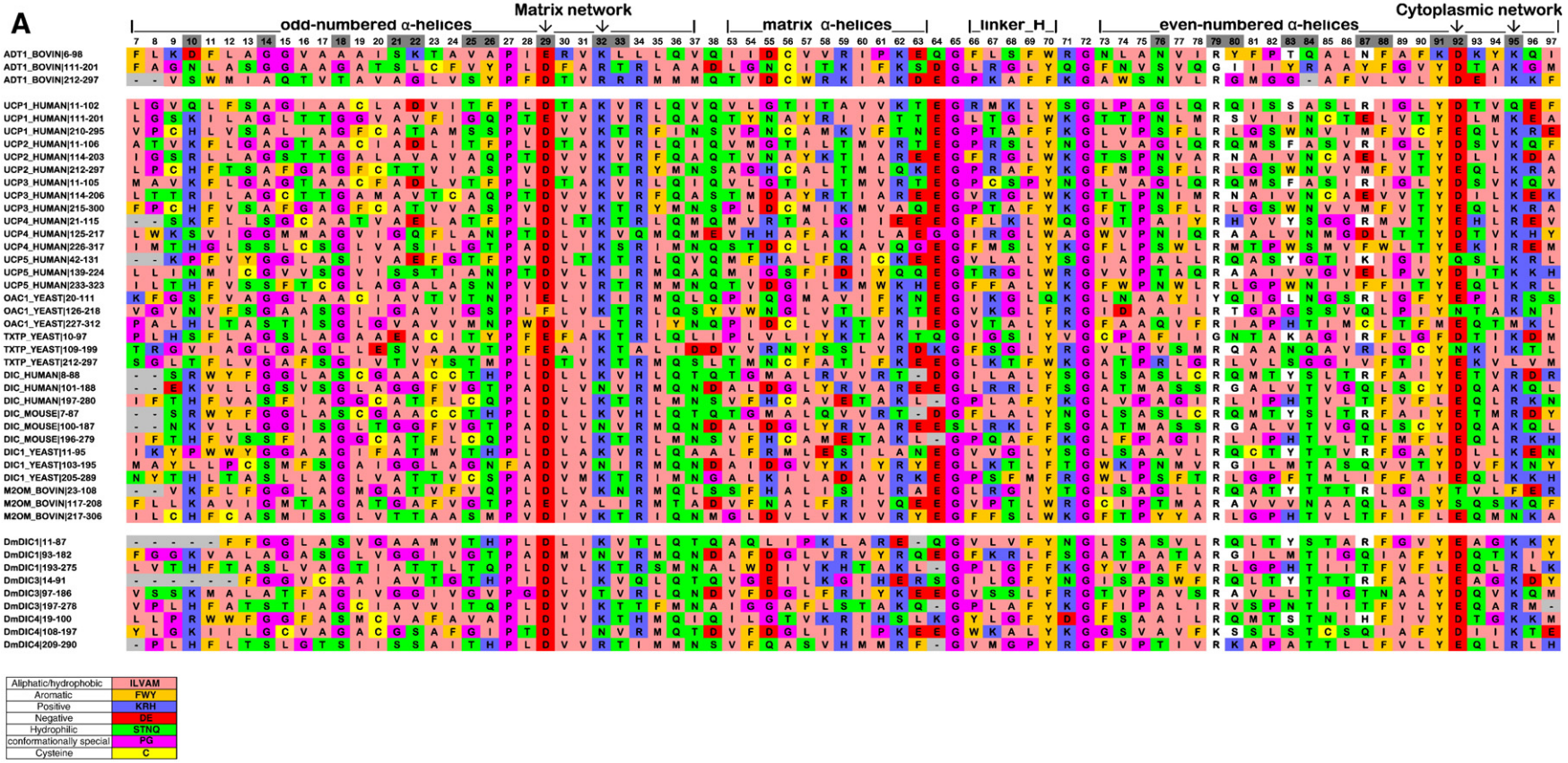

Fig. 3. A. Multiple alignments of sequence repeats of ADP/ATP, ketoacid carriers, and *Dm*Dics. The sequence repeats of *Dm*Dics are aligned towards those of the ADP/ATP and ketoacid carriers. Column numbers refer to numbering in the correspondent structure of the ADP/ATP carrier and are as in Robinson et al. [33]. Symmetry-related triplets in the cavity of the carriers are highlighted in grey, and residues in contact points (according to the definition of Robinson et al. [37]) are in white field. Topology derives from the ADP/ATP carrier (in odd-numbered alpha-helices, in matrix network, in matrix alpha-helices, in linkers, in even-numbered alpha-helices, and in cytoplasmic network). The residues are colored according to their physico-chemical properties as follows: aliphatic/hydrophobic (VILMA) in pink, aromatic (FWY) in orange, positive (KRH) in blue, negative (DE) in red, hydrophilic (STNQ) in green, cysteine in yellow, Glicine and Proline in magenta. B. Multiple alignments of sequence repeats of ADP/ATP, phosphate carriers, and *Dm*Dics. Typical phosphate carriers, including Q9XZE4_DROME, the phosphate carrier in *Drosophila melanogaster* (MPCP_DROME) are aligned with *Dm*Dics. Other explanations are as in panel A.

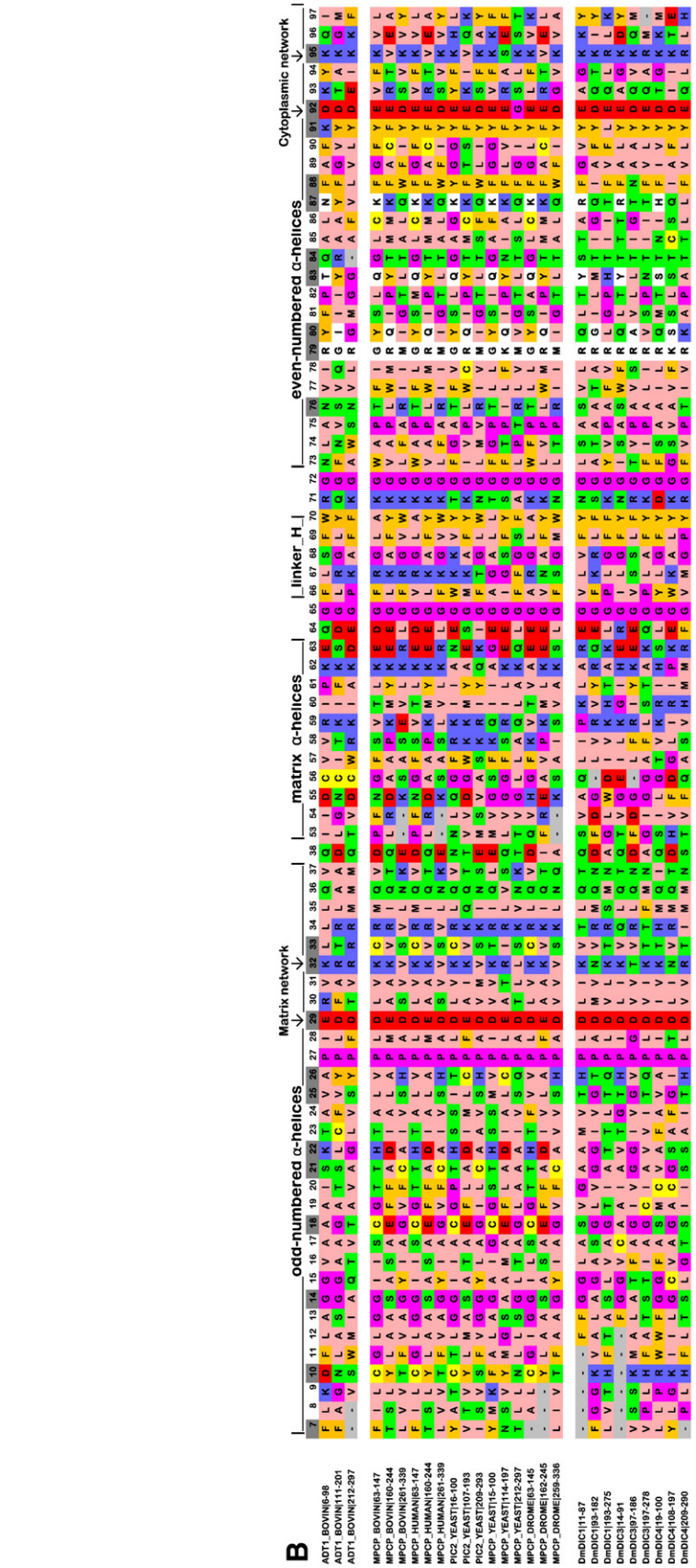

Fig. 3 (*continued*).

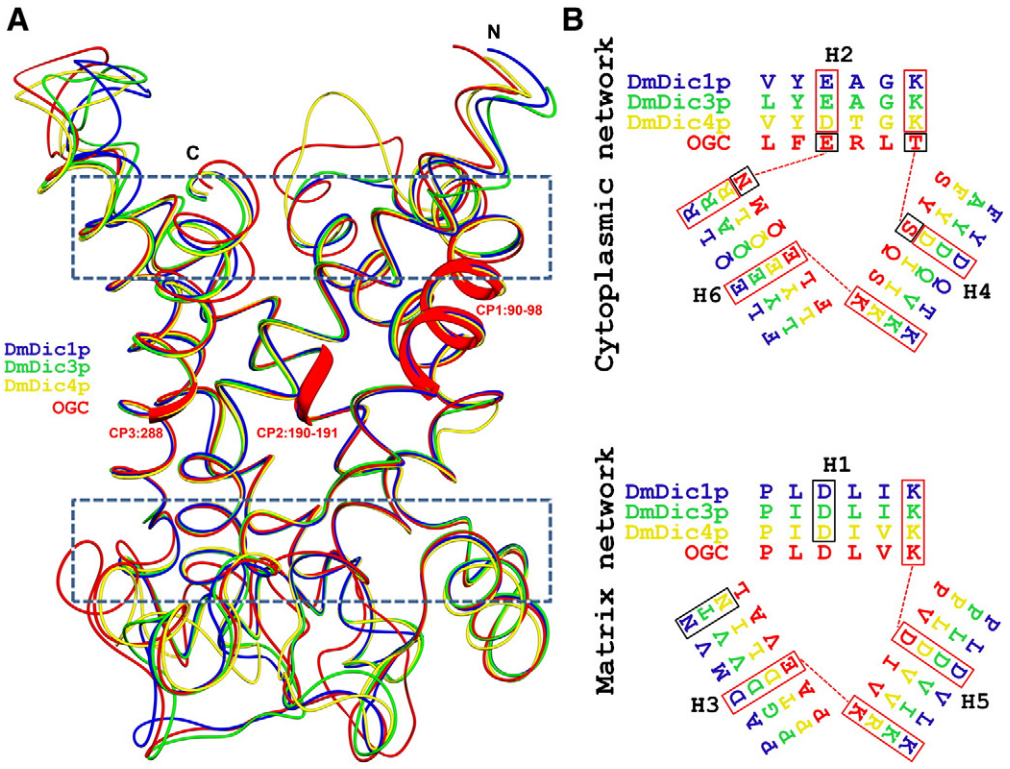

Fig. 4. A. Models of OGC and *Dm*Dic proteins. OGC, *Dm*Dic1p, *Dm*Dic3p, and *Dm*Dic4p are structurally aligned. Color code indicates the four different sequences. B. Matrix and cytoplasmic Networks of OGC and *Dm*Dics.

discussed above, it transports only phosphate, instead of malate for phosphate. The question then poses as to which extent this finding can be explained at a molecular level with the structural and mutagenesis data already described in literature and referring to site point mutations of OGC. Several regions have been detailed and mutated systematically in OGC [34,35,38]. These are all indicated for comparison in Table 4, where all the aligned residues of OGC, *Dm*Dic1p and *Dm*Dic3p, different from the contact points already addressed in Table 3, are now listed with their experimental annotation, when available. The *Dm*Dic1-3p carriers, which share 50% of identical residues among each other, conserved residues of the OGC in different positions. *Dm*Dic1p maintains L15, A16, L63, G79, Q172 identical to positions that in OGC have been shown to play a role in the transport activity. In *Dm*Dic3p, T78, T80, A107, and V120 are identical to their counterparts in OGC, and the experimental annotation of these residues also indicates proximity to important residues or loss of activity upon mutation (OGC V142). However, in regions that are important for OGC carrier activity, the following mutations are detected for the atypical *Dm*Dic3p: V17 in place of OGC L30, previously considered to be involved in structural changes; C18 in place of OGC A31, whose mutations promoted 50% of the loss in activity; A19 in place of G32 (the G32A mutation in OGC led to the loss of OGC transport activity); V23 in place of OGC T36, involved in substrate binding (interestingly in *Dm*Dic1p at this position an alanine instead of a valine is found); Q35 in place of OGC R48, involved in hydrogen bonding (also in this position the *Dm*Dic1p T33 is a better hydrogen donor than *Dm*Dic3p Q35); I67 in place of OGC L84, a position that is conserved in *Dm*Dic1p (in OGC the mutation L84I reduces 15% the transport activity); A83 instead of OGC G100 (loss of OGC transport activity was detected for the G100X mutation; interestingly this position is conserved in *Dm*Dic1p); T122 instead of OGC L144, not involved in hydrogen bonds; L172 instead of OGC V194; T174 instead of OGC Q198X, a mutation that induces loss of activity; E301X, again a mutation that induces loss of activity in OGC, is conserved in the *Dm*Dic1-3-4p.

Table 3
Mapping of OGC contact points onto *Dm*Dic carriers.

OGC	*Dm*Dic1p	*Dm*Dic3p	*Dm*Dic4p	Experimental annotation in OGC
R90	R69	R73	R82	Contact Point #1: R90 is conserved in all the sequences; Y94 and R98 are conserved only in *Dm*Dic1p and *Dm*Dic3p.
Y94	Y73	Y77	S86	
R98	R77	R81	H90	
R190	R164	R168	K179	Contact Point #2: R190 is conserved in *Dm*Dic1p and *Dm*Dic3p. In *Dm*Dic4p Arg is mutated in Lys. In OGC when the positive charged is preserved, the transport activity is lost (Stipani et al. [34,35,38]).
A191	G165	A169	S180	
R288	R257	R261	R272	Contact Point #3: all the sequences share the same residue.

Summing up, it appears that the conservation of contact points is a prerequisite for transport activity also in *Dm*Dic proteins. The conservation in flanking residues is also important in the typical activity of *Dm*Dic1p as shown in Table 4. When the putative binding site of OGC is considered [35,36], after structure alignment with both the typical and atypical dicarboxylate carriers of *D. melanogaster*, it appears that 67% of the aligned residues have higher steric hindrance in *Dm*Dic3p as compared with their counterparts of *Dm*Dic1p (difference in total residue volume of the flanking regions of the substrate binding sites in *Dm*Dic3p and *Dm*Dic1p is +137 Å^3, 18% higher in steric hindrance, Table 5). As a consequence, we suggest that phosphate is the only substrate that can be exchanged. This was computationally corroborated with flexible docking experiments of malate in the two substrate binding pockets of *Dm*Dic1p and *Dm*Dic3p that confirm the view that malate and phosphate are progressively loosing/increasing their stabilization from *Dm*Dic1p to *Dm*Dic3p due to decreasing/increasing of hydrogen bonding in the cavity (data not shown).

Table 4
Mapping of relevant residues of OGC onto *Dm*DIC1p and *Dm*DIC3p.

OGC	*Dm*Dic1p	*Dm*Dic3p	Experimental annotation in OGC
L30	L15 (conserved)	V17	MTSES or MTSET modifications are not tolerated, indicating that these modifications may interfere with protein structural changes (Cappello et al. [35,37])
A31	A16 (conserved)	C18	A31C reduces activity by 50% (Cappello et al. [35,37])
G32	S17	A19	Reduced transport activity when the mutation G32S occurs; no transport activity for the G32A mutation (Cappello et al. [35,37])
T36	A21	V23	Involved in specific substrate binding (Cappello et al. [35,37])
R48	T33	Q35	Involved in H-bonds (Kyungsun [45])
L84	L63 (conserved)	I67	L84I reduces transport activity by 15% (Cappello et al. [35,37])
T95	S74	T78 (conserved)	Proximal to contact point #1 (Cappello et al. [35,37])
T97	A76	T80 (conserved)	Proximal to contact point #1 (Cappello et al. [35,37])
G100	G79 (conserved)	A83	G100X induces complete loss of transport activity (Cappello et al. [35,37])
A129	S103	A107 (conserved)	Neighbor of contact point #2 (Cappello et al. [35,37])
V142	M116	V120 (conserved)	V142C induces loss of activity (Cappello et al. [35,37])
L144	N118	T122	No H-bonds occur in this position (Cappello et al [35,37])
V194	M168	L172	Dysfunction if mutated (Cappello et al. [35,37])
Q198	Q172 (conserved)	T176	Q198X induces complete loss of transport activity (Stipani et al. [35,37])
L199	I173	N177	Neighbor of contact point #2 (Cappello et al. [35,37])
T283	V252	I256	T283C partially reduces the activity (Cappello et al. [35,37])
E301	E270	E274	E301X induces complete loss of transport activity. This region was suggested to play a role in maintaining the stabilization of the alpha-helical bundle and protein structural integrity during conformational changes (Cappello et al. [35,37]).

4. Discussion

The study of the biochemical properties of *Dm*Dic proteins in reconstituted system (proteoliposomes) is a step towards understanding their specialized cellular functions. We used both theoretical and experimental methods for the characterization of these proteins.

In yeast and mammals, the dicarboxylate carrier is present as a single protein, while a screening of Flybase database revealed the presence of four dicarboxylate related proteins in *D. melanogaster*. A phylogenetic analysis carried out using the *D. melanogaster* Dic proteins revealed that *Dm*Dic1-4p are monophyletic and form a group with all Dics. On the basis of their homology with hDIC protein, they have been named *Dm*Dic1p, *Dm*Dic2p, *Dm*Dic3p, and *Dm*Dic4p. It is noteworthy that *Dm*Dic4p, sharing only 35% amino acid identity with hDIC, must be considered a dicarboxylate carrier since the most homolog carrier after hDIC is the human OGC with an identity of only 27%. Furthermore, the 35% identity falls within the same range as values obtained from comparisons of Dic sequences from diverse organisms. For example, protein sequence of hDIC is 36% identical to the *Saccharomyces cerevisiae* homolog [24].

Table 5
Conservations and mutations at the putative substrate binding site.

OGC	*Dm*DIC1p	*Dm*DIC3p
A35	A20 (conserved)	A22 (conserved)
T36	A21	V23
V39	T24	T26
Q40	H25	H27
R90 (CP#1)	**R69 (conserved)**	**R73 (conserved)**
Y94	**Y73 (conserved)**	**Y77 (conserved)**
T95	S74	T78 (conserved)
R98	**R77 (conserved)**	**R81 (conserved)**
A129	S103	A107 (conserved)
G130	G104 (conserved)	G108 (conserved)
G133	G107 (conserved)	G111 (conserved)
A134	G108	G112
R190 (CP#2)	**R164 (conserved)**	**R168 (conserved)**
A191	**G165**	**A169 (conserved)**
V194	M168	L172
N195	T169	T173
G230	G204 (conserved)	G208 (conserved)
T233	A207	A211
S237	T211	T215
T283	V252	I256
Y285	A254	A258
R288 (CP#3)	**R257 (conserved)**	**R261 (conserved)**
T293	T262 (conserved)	T266 (conserved)

Semi-quantitative RT-PCR analysis showed that *Dm*DIC1 is expressed in all developmental stages, *Dm*DIC2 is completely absent, whereas *Dm*DIC3 and *Dm*DIC4 expression is limited to the pupae stage. Furthermore, immune-fluorescence studies showed that *Dm*Dic1-3-4 proteins are localized in the mitochondrial compartment (data not shown).

We then characterized *Dm*Dic1p, *Dm*Dic3p, and *Dm*Dic4p biochemically. The substrate specificity and the kinetic characteristics of *Dm*Dic1p clearly show that this protein is the *D. melanogaster* homolog of the human dicarboxylate carrier. In this organism, the main role of *Dm*Dic1p could be gluconeogenesis from pyruvate rather than urea synthesis since this insect is uricotelic and converts most of its excess ammonia to uric acid via an arginase-independent pathway [39,40]. Another important function of the *Dm*Dic1p could be an anaplerotic one, i.e., it supplies substrates for the Krebs cycle to the mitochondrial matrix.

Interestingly, DmDic3p efficiently transports only phosphate, sulphate, and tiosulphate; however, its exclusive presence in the pupal stage, its low affinity for phosphate (Km 3.2 mM), and its low percent similarity with the known phosphate carriers (17.4%, 17.8%, and 18% similarity with the two human isoforms and yeast, respectively) led us to exclude that *Dm*Dic3p is the main *D. melanogaster* phosphate carrier necessary for the basal synthesis of mitochondrial ATP. Indeed it lacks the typical contact points of a mitochondrial phosphate carrier (Fig. 3B). It is endowed with three salt bridges in the cytoplasmic matrix instead of the two present in the phosphate carriers (Fig. 5), and this is in agreement with what previously suggested as a major indication of an exchange mechanisms more than a symport one [33]. Finally it should be remarked in the *D. melanogaster* genome are present two genes, CG4994 and CG9090, coding for two proteins with high percentage of similarity with the human [41] (ranging from 62% to 64%) and yeast [42] (ranging from 31% to 32%) phosphate carriers. One of these is included in Figs. 3B and 5. We therefore conclude that *Dm*Dic3p does not accomplish the basic energy requirement but becomes active to accommodate the higher energy demands associated with larval-to-adult metamorphosis, which occurs during the pupal phase [43], the only developmental stage in which the protein is expressed.

All these data, together with our structural/functional analysis, support the following final considerations. *Dm*Dic1p shows a typical mitochondrial dicarboxylate carrier exchange activity and consequently this can be correlated at a molecular level with the conservation at CP1

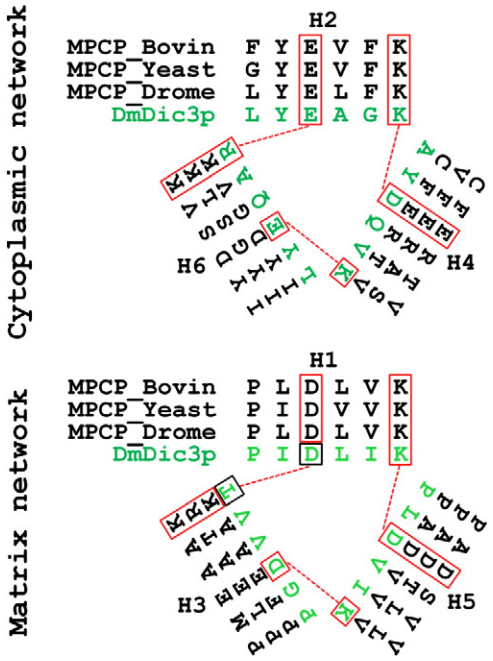

Fig. 5. Models of OGC and *Dm*Dic proteins. MPCP_BOVIN, MPCP_YEAST, MPCP_DROME (phosphate carriers), and *Dm*Dic3p are structurally aligned. In black and green are indicated, respectively, the three phosphate carriers and *Dm*Dic3p sequences.

of the typical structural R-Y-R motif in H2 of the ketoacid carriers previously described. The flanking side chains in this region of *Dm*Dic1p when compared to that in OGC Y show some changes (A93toL, T97toA) that may correlate with the different substrate exchanged by the two carriers (malate vs. phosphate and malate vs. 2-oxoglutarate). The atypical *D. melanogaster* carrier in this region shows a higher conservation of residues with OGC than *Dm*Dic1p (only an A93toL is noticeable). As to the non-active *Dm*Dic4p the R–Y–R motif is absent, being both OGC Y94 and R98 substituted with S and H, respectively, suggesting that the loss of conserved residues in this position is relevant to the lack of activity of *Dm*Dic4p.

At CP2 in H4, it appears that the OGC motif RA is conserved only in *Dm*Dic3p that transport only phosphate, whereas the typical carrier *Dm*Dic1p, while conserving R is endowed with a G in the flanking region. The motif is not conserved in *Dm*Dic4p (OGC RA is KS). This corroborates the view that R in this position is crucial in modulating activity also in the *Dm*Dic subfamily.

At CP3 in H6 OGC R288 is conserved in all the three *D. melanogaster* proteins, suggesting that this is rather a general marker of the carrier family than a marker of specific activity. The carrier motif signature P–X– [DE] –X–X[RK] is conserved in H1 and H5 and partially conserved in H3 in all 4 sequences, rather independently of the different functions. The sequence motif [YWLF] – [KR] –G–X–X–P present in H4 of OCG is conserved at the same position of *Dm*Dic3p. In *Dm*Dic1p and *Dm*Dic4p an A and a V apparently occurs instead of a P. In H6 the same motif is again highly conserved in all the sequences. Finally the thoroughly mutated segment in H4 of OGC, with the exception of CP2 and flanking regions already commented upon above, seems to have little counterpart as a whole in the corresponding three Dics regions. Other residues relevant on the matrix site binding regions are fairly well conserved in Matrix patch 1 and 2, as previously described [34] and poorly conserved in the remaining residues. This is so rather irrespectively of the organism source and carrier function. Furthermore and more interestingly, the loss of malate/phosphate exchange is due to a higher steric hindrance of the mutated residues in transport path of *Dm*Dic3p as compared to *Dm*Dic1p (Table 5).

In conclusion, taking into account the kinetic characteristics and the structural data, *Dm*Dic1p seems to be a typical dicarboxylate carrier operating during gluconeogenesis, whereas *Dm*Dic3p seems to be its paralog. *Dm*Dic3p during evolution could have lost the ability to transport the dicarboxylate and conserved that to transport phosphate, this latter necessary in high amount for the ATP synthesis during the metamorphosis.

The inability of *Dm*Dic4p to transport both dicarboxylate and phosphate could be explained by the lack of selective pressure upon this gene copy, probably arisen from a duplication of the *Dm*DIC ancestral gene [44]; therefore, *Dm*DIC4 could have been free to mutate and acquire a new function, which remains to be determined.

Acknowledgments

This article is dedicated to the memory of Giancarlo Mazzeo, Ph.D., whose scientific contribution has been fundamental. He deserves our deepest gratitude.

References

[1] F. Palmieri, The mitochondrial transporter family (SLC25): physiological and pathological implications, Pflugers Arch. 447 (2004) 689–709.
[2] C. Carrisi, M. Madeo, P. Morciano, V. Dolce, G. Cenci, A.R. Cappello, G. Mazzeo, D. Iacopetta, L. Capobianco, Identification of the *Drosophila melanogaster* mitochondrial citrate carrier: bacterial expression, reconstitution, functional characterization and developmental distribution, J. Biochem. 144 (2008) 389–392.
[3] R. Rikhy, M. Ramaswami, K.S. Krishnan, A temperature-sensitive allele of *Drosophila* sesB reveals acute functions for the mitochondrial adenine nucleotide translocase in synaptic transmission and dynamin regulation, Genetics 165 (2003) 1243–1253.
[4] M.D. Brand, J.L. Pakay, A. Ocloo, J. Kokoszka, D.C. Wallace, P.S. Brookes, E.J. Cornwall, The basal proton conductance of mitochondria depends on adenine nucleotide translocase content, Biochem. J. 392 (2005) 353–362.
[5] Y.W. Fridell, A. Sanchez-Blanco, B.A. Silvia, S.L. Helfand, Functional characterization of a *Drosophila* mitochondrial uncoupling protein, J. Bioenerg. Biomembr. 36 (2004) 219–228.
[6] N.A. Oey, L. Ijlst, C.W. van Roermund, F.A. Wijburg, R.J. Wanders, dif-1 and colt, both implicated in early embryonic development, encode carnitine acylcarnitine translocase, Mol. Genet. Metab. 85 (2005) 121–124.
[7] C. Metzendorf, W. Wu, M.I. Lind, Overexpression of *Drosophila* mitoferrin in l(2) mbn cells results in dysregulation of Fer1HCH expression, Biochem. J. 421 (2009) 463–471.
[8] D. Iacopetta, C. Carrisi, G. De Filippis, V.M. Calcagnile, A.R. Cappello, A. Chimento, R. Curcio, A. Santoro, A. Vozza, V. Dolce, F. Palmieri, L. Capobianco, The biochemical properties of the mitochondrial thiamine pyrophosphate carrier from *Drosophila melanogaster*, FEBS J. 277 (2010) 1172–1181.
[9] F. Palmieri, G. Prezioso, E. Quagliariello, M. Klingenberg, Kinetic study of the dicarboxylate carrier in rat liver mitochondria, Eur. J. Biochem. 22 (1971) 66–74.
[10] R.N. Johnson, J.B. Chappell, The transport of inorganic phosphate by the mitochondrial dicarboxylate carrier, Biochem. J. 134 (1973) 769–774.
[11] M. Crompton, F. Palmieri, M. Capano, E. Quagliariello, The transport of thiosulphate in rat liver mitochondria, FEBS Lett. 46 (1974) 247–250.
[12] M. Crompton, F. Palmieri, M. Capano, E. Quagliariello, The transport of sulphate and sulphite in rat liver mitochondria, Biochem. J. 142 (1974) 127–137.
[13] W.A. Coty, P.L. Pedersen, Phosphate transport in rat liver mitochondria. Kinetics, inhibitor sensitivity, energy requirements, and labeled components, Mol. Cell. Biochem. 9 (1975) 109–124.
[14] R.S. Kaplan, P.L. Pedersen, Isolation and reconstitution of the n-butylmalonate-sensitive dicarboxylate transporter from rat liver mitochondria, J. Biol. Chem. 260 (1985) 10293–10298.
[15] F. Bisaccia, C. Indiveri, F. Palmieri, Purification and reconstitution of two anion carriers from rat liver mitochondria: the dicarboxylate and the 2-oxoglutarate carrier, Biochim. Biophys. Acta 933 (1988) 229–240.
[16] J. Lancar-Benba, B. Foucher, M. Saint-Macary, Purification of the rat-liver mitochondrial dicarboxylate carrier by affinity chromatography on immobilized malate dehydrogenase, Biochim. Biophys. Acta 1190 (1994) 213–216.
[17] J. Lancar-Benba, B. Foucher, M. Saint-Macary, Characterization, purification and properties of the yeast mitochondrial dicarboxylate carrier (*Saccharomyces cerevisiae*), Biochimie 78 (1996) 195–200.
[18] C. Indiveri, G. Prezioso, T. Dierks, R. Kramer, F. Palmieri, Kinetic characterization of the reconstituted dicarboxylate carrier from mitochondria: a four-binding-site sequential transport system, Biochim. Biophys. Acta 1143 (1993) 310–318.
[19] G. Fiermonte, L. Palmieri, V. Dolce, F.M. Lasorsa, F. Palmieri, M.J. Runswick, J.E. Walker, The sequence, bacterial expression, and functional reconstitution of the rat mitochondrial dicarboxylate transporter cloned via distant homologs in yeast and Caenorhabditis elegans, J. Biol. Chem. 273 (1998) 24754–24759.
[20] L. Palmieri, F. Palmieri, M.J. Runswick, J.E. Walker, Identification by bacterial expression and functional reconstitution of the yeast genomic sequence

encoding the mitochondrial dicarboxylate carrier protein, FEBS Lett. 399 (1996) 299–302.
[21] D. Kakhniashvili, J.A. Mayor, D.A. Gremse, Y. Xu, R.S. Kaplan, Identification of a novel gene encoding the yeast mitochondrial dicarboxylate transport protein via overexpression, purification, and characterization of its protein product, J. Biol. Chem. 272 (1997) 4516–4521.
[22] R. Krämer, F. Palmieri, Metabolite Carriers in Mitochondria, Elsevier Science Publishers B.V., Amsterdam, 1992.
[23] L. Palmieri, A. Vozza, A. Honlinger, K. Dietmeier, A. Palmisano, V. Zara, F. Palmieri, The mitochondrial dicarboxylate carrier is essential for the growth of *Saccharomyces cerevisiae* on ethanol or acetate as the sole carbon source, Mol. Microbiol. 31 (1999) 569–577.
[24] G. Fiermonte, V. Dolce, R. Arrigoni, M.J. Runswick, J.E. Walker, F. Palmieri, Organization and sequence of the gene for the human mitochondrial dicarboxylate carrier: evolution of the carrier family, Biochem. J. 344 (Pt 3) (1999) 953–960.
[25] V. Dolce, P. Scarcia, D. Iacopetta, F. Palmieri, A fourth ADP/ATP carrier isoform in man: identification, bacterial expression, functional characterization and tissue distribution, FEBS Lett. 579 (2005) 633–637.
[26] V. Dolce, G. Fiermonte, M.J. Runswick, F. Palmieri, J.E. Walker, The human mitochondrial deoxynucleotide carrier and its role in the toxicity of nucleoside antivirals, Proc. Natl Acad. Sci. USA 98 (2001) 2284–2288.
[27] F. Palmieri, C. Indiveri, F. Bisaccia, V. Iacobazzi, Mitochondrial metabolite carrier proteins: purification, reconstitution, and transport studies, Methods Enzymol. 260 (1995) 349–369.
[28] P.L. Martelli, P. Fariselli, R. Casadio, An ENSEMBLE machine learning approach for the prediction of all-alpha membrane proteins, Bioinformatics 19 (Suppl 1) (2003) i205–i211.
[29] N. Eswar, B. Webb, M.A. Marti-Renom, M.S. Madhusudhan, D. Eramian, M.Y. Shen, U. Pieper, A. Sali, Comparative protein structure modeling using Modeller, Curr. Protoc. Bioinform. (2006), Chapter 5, Unit 5 6.
[30] E. Pebay-Peyroula, C. Dahout-Gonzalez, R. Kahn, V. Trezeguet, G.J. Lauquin, G. Brandolin, Structure of mitochondrial ADP/ATP carrier in complex with carboxyatractyloside, Nature 426 (2003) 39–44.
[31] R.A. Laskowski, M.W. MacArthur, D.S. Moss, J.M. Thornton, PROCHECK: a program to check the stereochemical quality of protein structures, J. Appl. Cryst. 26 (1993) 283–291.
[32] M.J. Sippl, Recognition of errors in three-dimensional structures of proteins, Proteins 17 (1993) 355–362.
[33] A.J. Robinson, C. Overy, E.R. Kunji, The mechanism of transport by mitochondrial carriers based on analysis of symmetry, Proc. Natl Acad. Sci. USA 105 (2008) 17766–17771.
[34] B. Morozzo Della Rocca, D.V. Miniero, G. Tasco, V. Dolce, M. Falconi, A. Ludovico, A.R. Cappello, P. Sanchez, I. Stipani, R. Casadio, A. Desideri, F. Palmieri, Substrate-induced conformational changes of the mitochondrial oxoglutarate carrier: a spectroscopic and molecular modelling study, Mol. Membr. Biol. 22 (2005) 443–452.
[35] A.R. Cappello, R. Curcio, D. Valeria Miniero, I. Stipani, A.J. Robinson, E.R. Kunji, F. Palmieri, Functional and structural role of amino acid residues in the even-numbered transmembrane alpha-helices of the bovine mitochondrial oxoglutarate carrier, J. Mol. Biol. 363 (2006) 51–62.
[36] A.R. Cappello, D.V. Miniero, R. Curcio, A. Ludovico, L. Daddabbo, I. Stipani, A.J. Robinson, E.R. Kunji, F. Palmieri, Functional and structural role of amino acid residues in the odd-numbered transmembrane alpha-helices of the bovine mitochondrial oxoglutarate carrier, J. Mol. Biol. 369 (2007) 400–412.
[37] A.J. Robinson, E.R. Kunji, Mitochondrial carriers in the cytoplasmic state have a common substrate binding site, Proc. Natl Acad. Sci. USA 103 (2006) 2617–2622.
[38] V. Stipani, A.R. Cappello, L. Daddabbo, D. Natuzzi, D.V. Miniero, I. Stipani, F. Palmieri, The mitochondrial oxoglutarate carrier: cysteine-scanning mutagenesis of transmembrane domain IV and sensitivity of Cys mutants to sulfhydryl reagents, Biochemistry 40 (2001) 15805–15810.
[39] M.L. Samson, *Drosophila* arginase is produced from a nonvital gene that contains the elav locus within its third intron, J. Biol. Chem. 275 (2000) 31107–31114.
[40] G. Pesole, M.P. Bozzetti, C. Lanave, G. Preparata, C. Saccone, Glutamine synthetase gene evolution: a good molecular clock, Proc. Natl Acad. Sci. USA 88 (1991) 522–526.
[41] V. Dolce, V. Iacobazzi, F. Palmieri, J.E. Walker, The sequences of human and bovine genes of the phosphate carrier from mitochondria contain evidence of alternatively spliced forms, J. Biol. Chem. 269 (1994) 10451–10460.
[42] A. Phelps, C.T. Schobert, H. Wohlrab, Cloning and characterization of the mitochondrial phosphate transport protein gene from the yeast Saccharomyces cerevisiae, Biochemistry 30 (1991) 248–252.
[43] K.a.R.N.S. Singh, Metamorphosis of the central nervous system of *Drosophila melanogaster* Meigen (Diptera: Drosophilidae) during pupation, J. Biosci. 24 (1999) 345–360.
[44] A. Wagner, The fate of duplicated genes: loss or new function? Bioessays 20 (1998) 785–788.
[45] K. Kyungsun, R.A. Friesner, Hydrogen bonding between amino acid backbone and side chain analogues: a high level ab Initio study, J. Am. Chem. Soc. 119 (52) (1997) 12952–12961.